Neurosci Bull October 1, 2012, 28(5): 483–492. http://www.neurosci.cn
DOI: 10.1007/s12264-012-1257-z

·Original Article·

Endophilin isoforms have distinct characteristics in interactions with N-type Ca^{2+} channels and dynamin I

Qi Tian[1], Ji-Feng Zhang[1], Jinjin Fan[2], Zhihong Song[3], Yuan Chen[1]

[1]*Center for Neurobiology, Zhongshan School of Medicine,* [2]*Department of Nephrology, The First Affiliated Hospital,*
[3]*Department of Biochemistry, Zhongshan School of Medicine, Sun-Yat Sen University, Guangzhou 510080, China*

Abstract: **Objective** Formation of the endophilin II-Ca^{2+} channel complex is Ca^{2+}-dependent in clathrin-mediated endocytosis. However, little is known about whether the other two endophilin isoforms have the same features. The present study aimed to investigate the characteristics of the interactions of all three isoforms with Ca^{2+} channels and dynamin I. **Methods** N-type Ca^{2+} channel C-terminal fragments (NCFs) synthesized with a ^{3}H-leucine-labeled kit, were incubated with endophilin-GST fusion proteins, followed by pull-down assay. Results were counted on a scintillation counter. In addition, the different endophilin isoforms were each co-transfected with dynamin I into 293T cells, followed by flow cytometry and co-immunoprecipitation assay. Immunostaining was performed and an image analysis program was used to evaluate the overlap coefficient of cells expressing endophilin and dynamin I. **Results** All three isoforms interacted with NCF. Endophilins I and II demonstrated clear Ca^{2+}-dependent interactions with NCF, whereas endophilin III did not. Co-immunoprecipitation showed that, compared to endophilin I/II, the interaction between endophilin III and dynamin I was significantly increased. Similar results were obtained from flow cytometry. Furthermore, endophilin III had a higher overlap coefficient with dynamin I in co-transfected 293T cells. **Conclusion** Endophilin isoforms have distinct characteristics in interactions with NCF and dynamin I. Endophilin III binding to NCF is Ca^{2+}-independent, implying that it plays a different role in clathrin-mediated endocytosis.

Keywords: endophilin; Ca^{2+}; dynamin I; endocytosis; proline-rich domain; SH3 domain

1 Introduction

Endophilin is one of the major endocytic proteins that contains an Src homology 3 (SH3) domain. Studies have shown that three types of endophilin exist in rats: endophilin I is expressed only in brain, endophilin II in multiple tissues, and endophilin III mainly in brain, testis and thymus[1-3]. Endophilins I and II also form dimers through a coiled-coil domain[4-7]. All three isoforms are concentrated in presynaptic nerve terminals[8-10], and play important roles in synaptic vesicle recycling in neurons[11,12].

Endophilin is a conserved protein containing two functional domains: an N-terminal Bin-amphiphysin-Rvs (BAR) domain and a C-terminal SH3 domain[13]. The N-terminus mainly participates at the base of the membrane invagination in clathrin-coated endocytosis[14-16]. In brain, the SH3 domain interacts selectively with proteins containing a proline-rich domain (PRD), such as synaptojanin, amphiphysin and GTPase dynamin[17-22]. Our previous studies found an atypical PRD embedded within endophilin II,

Corresponding author: Yuan Chen
Tel & Fax: +86-20-87332238
E-mail: cheny33@mail.sysu.edu.cn
Article ID: 1673-7067(2012)05-0483-10
Received date: 2012-02-24; Accepted date: 2012-05-10

and Ca^{2+} binds to endophilin II directly and regulates endophilin-Ca^{2+} channel complexes[23]. Endophilin II has two different modes at different Ca^{2+} concentrations. At low Ca^{2+} concentration (100–300 nmol/L), endophilin II forms an open mode, the SH3 domain is exposed, and the interactions between endophilin II and its target proteins are increased. When the Ca^{2+} level increases (>1 μmol/L), the endophilin II SH3 domain may have an intramolecular interaction with its embedded PRD domain. In this situation, endophilin II changes to a closed mode and is no longer available for either Ca^{2+} channels or dynamin, which leads to its Ca^{2+}-dependence[23]. However, whether the other two isoforms of endophilin have similar characteristics in Ca^{2+}-dependent binding with Ca^{2+} channel proteins and whether these three isoforms have distinct interactions with dynamin I in clathrin-mediated endocytosis remain unknown. This study aimed to resolve these issues.

2 Materials and methods

2.1 Construction of plasmids Total RNA was extracted from the adult Sprague-Dawley rat brain using an RNeasy Mini Kit (Qiagen, Valencia, CA) and first-strand cDNA was generated by Superscript II reverse transcriptase (Life Technologies, Grand Island, NY). Target DNA fragments were amplified by RT-PCR using primers designed and synthetized according to the GenBank Database (Table 1). The full-length endophilin cDNA was inserted into the pGEX-4-T1 (Amersham Pharmacia Biotech, Piscataway, NJ) and pEGFP-C2 vectors (Clontech, Mountain View, CA). Dynamin I cDNA was cloned into the pCMV-Tag5 vector (Stratagene, Santa Clara, CA). The full-length N-type Ca^{2+} channel C-terminal fragment (NCF) cDNA was ligated into a pSP72 vector (Promega, Madison, WI). All constructs were verified by sequencing. The GST-endophilins were used for GST fusion protein pull-down assays. pEGFP-endophilin and dynamin I were used for detecting their co-expression in 293T cells. NCF was used for ^{3}H-leucine-labeled synthesized proteins by an *in vitro* translation kit (Promega).

2.2 Expression and purification of recombinant GST-fusion proteins To purify GST-fused proteins, GST-endophilin isoform constructs were transformed into the BL21 (DE3) strain of *Escherichia coli* (Invitrogen, Grand Island, NY). Production of fusion proteins was induced by incubation with 0.2 mmol/L isopropyl-1-thio-b-d-galactopyranoside for 3 h at 30°C. Cells were spun down and resuspended in a buffer containing (in mmol/L) 30 NaCl, 30 Tris, 0.2 EDTA, 1 DTT, pH 8.0, along with a cocktail of protease inhibitors (Merck, Whitehouse Station, NJ). The cell suspension was treated with 0.1% lysozyme followed by 0.5% deoxycholic acid on ice for 20 min. After sonication, the cell debris was removed by centrifugation (15 000 g for 30 min). The supernatant, with 1% Triton X-100, was

Table 1. Primers used in RT-PCR

Genes (GenBank accession No.)	Sequences of primers	Restriction enzyme sites
Dynamin I	Forward TATGTCGACATGGGCAACCGCGGC	Hind III
(NM080689)	Reverse TAAGCGGCCGCTCAGGGGTCACTGAT	Xhol I
Endophilin I	Forward ATAGAATTCATGTCGGTGGCGGGG	EcoR I
(AF009603)	Reverse TAAGTCGACCTAATGGGGCAGAGC	Sal I
Endophilin II	Forward ATAGAATTCATGTCGGTGGCGGGG	EcoR I
(AF009602)	Reverse TAAGTCGACTCACTGAGGCAGAGG	Sal I
Endophilin III	Forward ATAGAATTCATGTCGGTGGCGGGG	EcoR I
(AF009604)	Reverse ACTGTCGACTTACCGAGGTAAAGG	Sal I
NCF	Forward TGGTACCGAAGCTACTTCCGGT	Kpn I
(M94172)	Reverse TGATATCCAGCAGACATGGGGC	EcoR V

used for the purification of the GST fusion proteins using glutathione-Sepharose beads.

2.3 GST-fusion protein pulldown assays Pulldown assays were carried out as previously described[23]. Briefly, ^{3}H-labeled NCF proteins were synthesized *in vitro* using the TNT Coupled Reticulocyte Lysate System (Promega). The assay buffer contained 100 mmol/L NaCl, 20 mmol/L Tris-HCl, and 5% glycerol (pH 7.0) along with 1% Triton X-100 and a cocktail of protease inhibitors (Merck). Approximately 5 g GST-fused protein was incubated with 2 μL ^{3}H-labeled protein with gentle rocking at 4°C overnight. The results were analyzed by a scintillation counter (Beckman, Brea, CA). To minimize the variability of radioactivity between experiments, counts per minute values were normalized to that in the presence of 300 nmol/L Ca^{2+} for each endophilin isoform analysis. A computer program (http://www.stanford.edu/cpatton/maxc.html) was used to prepare Ca^{2+} solutions at low concentrations.

2.4 Cell culture and transfection 293T cells were grown in Dulbecco's modified Eagle's medium supplemented with 10% fetal bovine serum and 100 units/mL penicillin and streptomycin (Invitrogen) in a 5% CO_2, 37°C incubator (Thermo Scientific, Asheville, NC). For immunostaining assays, 293T cells were grown on 12-mm circular coverslips and transfected using the calcium-phosphate transfection method (Myc-dynamin I and EGFP-endophilin I/II/III at the ratio of 1:2). For immunoprecipitation, 2 μg Myc-dynamin I and 4 μg EGFP-endophilin I/II/III (1:2) were cotransfected into 50%–70% confluent 293T cells on 100-mm culture dishes by the calcium-phosphate transfection method. For flow cytometric analysis of the localization of endophilin and dynamin I, 4 μg EGFP-endophilin I/II/III and Myc-dynamin I (1:1) were cotransfected into 80%–90% confluent cells using Lipofectamine^{TM}2000. EGFP-tag, Myc-tag, EGFP-endophilin, Myc-dynamin I and blank 293T were used as negative controls for flow cytometry.

2.5 Immunostaining assay The transfected 293T cells described above were washed in PBS, fixed with 4% (*w*/*v*) paraformaldehyde (Sigma, St. Louis, MO) for 5 min at room temperature, and permeabilized with 0.1% Triton X-100 in PBS for 20 min. Cells were blocked in 3% normal donkey serum in TBS + 0.1% TritonX-100 for 1 h at room temperature, incubated with mouse anti-dynamin antibody (Clontech, Mountain View, CA; 1:600) at 4°C overnight, washed 3 times for 10 min with PBS + 0.1% Tween20, and then incubated with monoclonal donkey anti-mouse IgG Dylight 549 (Jackson, West Grove, PA; 1:500) for 2 h at room temperature. After three washes, cells were mounted onto glass slides with Fluoro Gel II, containing DAPI (EMS, Hatfield, PA). Microscopy and image analysis were carried out at the same optical slice thickness in every channel (488-nm laser 1 AU = 0.7 μm, 543-nm laser 0.71 AU = 0.7 μm) using a confocal microscope (LSM 710; Carl Zeiss, Germany). Mander's coefficient was used to measure colocalization[24,25]. One-way ANOVA was used for statistical comparisons.

2.6 Co-immunoprecipitation (co-IP) and immunoblotting Proteins were extracted from transfected 293T cells using 1 mL lysis buffer containing (in mmol/L) 137 NaCl, 2.7 KCl, 4.3 Na_2HPO_4, 1.4 KH_2PO_4, 5.0 EDTA, 5.0 EGTA, 1.0 PMSF, 1% Triton X-100, and protease inhibitor cocktail (Merck) on ice for 30 min. The lysate underwent 12 passes through a 25-gauge needle, then was centrifuged at 17 000 g for 30 min at 4°C. The supernatant was incubated for 8 h at 4°C with 50 μL protein G Plus/Protein A-Agarose (Merck) that had been pre-incubated with 5 μg mouse anti-dynamin for 1 h at 4°C. The immunoprecipitates were washed three times at 4°C with 1 mL PBS containing 0.5% Triton X-100. Protein G beads carrying the immune complexes were collected after each wash by centrifugation at 17 000 g for 3 min.

For immunoblotting, all supernatants were loaded onto a 10% SDS-PAGE gel. The separated proteins were transferred onto polyvinylidene difluoride membranes (Pierce, Rockford, IL). The membranes were blocked with 5% non-fat milk in TBS and 0.1% Tween-20, and then incubated with anti-endophilin I-III (Santa Cruz Biotechnology, Santa Cruz, CA) (1:1 000), anti-dynamin (1:1 000) or anti-GAPDH (1:2 000) antibody overnight at 4°C. After 3–4 washes with TBS and 0.1% Tween 20 (10 min/wash at room temperature), membranes were incubated with horseradish peroxidase-conjugated secondary antibody.

Protein bands were detected by developing blots using an ECL kit (Pierce). The band densities were quantified with Image J (NIH, USA). Density ratios of dynamin I/GAPDH and Endo/GAPDH were used for each endophilin isoform analysis, to minimize variability.

2.7 Flow cytometry Transfected 293T cells were harvested and digested with 0.05% trypsin, fixed in 4% paraformaldehyde for 40 min, and permeabilized by 0.1% Triton X-100 for 30 min on ice. After 600 g centrifugation for 5 min at 4°C, cells were blocked in 3%–5% bovine serum albumin, and stained with sequential anti-dynamin antibody and phycoerythrin (PE)-conjugated rat anti-mouse IgG1 antibody (BD Transduction Laboratories, San Jose, CA) at room temperature for 30 min. After washing and resuspending in 300 μL PBS, cells were evaluated by flow cytometry.

2.8 Statistical analysis Data are presented as mean ± SEM. Statistical comparisons were assessed with one-way ANOVA followed by Bonferroni or Tamhane *post hoc* test (shown below). P <0.05 was considered as statistically significant.

3 Results

3.1 Diverse effects of Ca^{2+} in regulating endophilin isoform interaction with N-type Ca^{2+} channel C-terminal Our previous studies showed that the endophilin II-Ca^{2+} channel interaction is Ca^{2+}-dependent, and formation of the complex is readily reversible at high [Ca^{2+}][23]. To estimate whether Ca^{2+} affects formation of the endophilin isoform-Ca^{2+} channel complexes, we constructed the recombinants of endophilin-GST and NCF-pSP72 (Fig. 1A). The GST-fusion endophilin isoforms were purified well (Fig. 1B); although slight bands below the predicted size were also detected, they were still identified to be endophilins and did not affect the results (detected by Western blot using endophilin antibodies, data not shown). Besides, the autoradiography results showed a specific production of ^{3}H-labeled NCF, although there were mixed bands when 4-μL samples were used (Fig. 1C). We thus used 2-μL products for the subsequent experiments to reduce interference. GST pulldown assay was performed under the indicated [Ca^{2+}] as previously described[23]. All three endophilin isoforms interacted with NCF (Fig. 1D). For endophilin II, binding to Ca^{2+} channels was enhanced when [Ca^{2+}] was increased from 0 to 300 nmol/L. The optimal concentration for formation of the endophilin II-Ca^{2+} channel complex was 100–300 nmol/L. When [Ca^{2+}] was increased to 1 μmol/L, the binding was significantly reduced to 69.00 ± 1.50% of that in the presence of 300 nmol/L Ca^{2+} (n = 4, P = 0.009). This Ca^{2+}-dependent binding pattern was similar to our previous report[23], and was also obtained for endophilin I, but it was slightly degraded at 0 nmol/L. Both endophilins I and II had the optimal [Ca^{2+}] at 100–300 nmol/L (significant differences at indicated [Ca^{2+}]; n = 4, P <0.01, Fig. 1D). Interestingly, in comparison to endophilin II, endophilin III showed a Ca^{2+}-independent pattern of interaction with NCF. The normalized count ratio without Ca^{2+} was 81.00 ± 31.00%, with Ca^{2+} at 100 nmol/L was 111.00 ± 24.00%, and at 1 μmol/L was 109.00 ± 24.00% that at 300 nmol/L (no statistically significant difference, n = 4).

3.2 Colocalization of endophilin isoforms and dynamin I in 293T cells As dynamin interacts with endophilin[18,20] and plays important roles in clathrin-mediated endocytosis[26-29], we used immunostaining to investigate whether the interactions between dynamin and the three endophilin isoforms have the same characteristics. All three endophilins colocalized with dynamin I (Fig. 2A). To reveal potentially different degrees of colocalization among the endophilins, we further analyzed the overlap coefficient in every cell that expressed both endophilin and dynamin I. Images of immunostaining were collected and colocalization was determined by the overlap coefficients[24,25]. Endophilin III was more highly colocalized with dynamin I (0.95 ± 0.03, n = 30) than endophilin I/II (I, 0.91 ± 0.05; II, 0.92 ± 0.05; n = 30, P <0.01 for both, Fig. 2B). These results show that endophilin III interacts more with dynamin I than endophilin I/II.

3.3 Interactions of dynamin I with endophilin I/II/III To further confirm the immunostaining data, another two approaches were used. The co-IP results showed that, compared with endophilin I/II, endophilin III immunoprecipitated more dynamin I (Fig. 3B). The density ratios of endophilin I-II/GAPDH bands were significantly lower

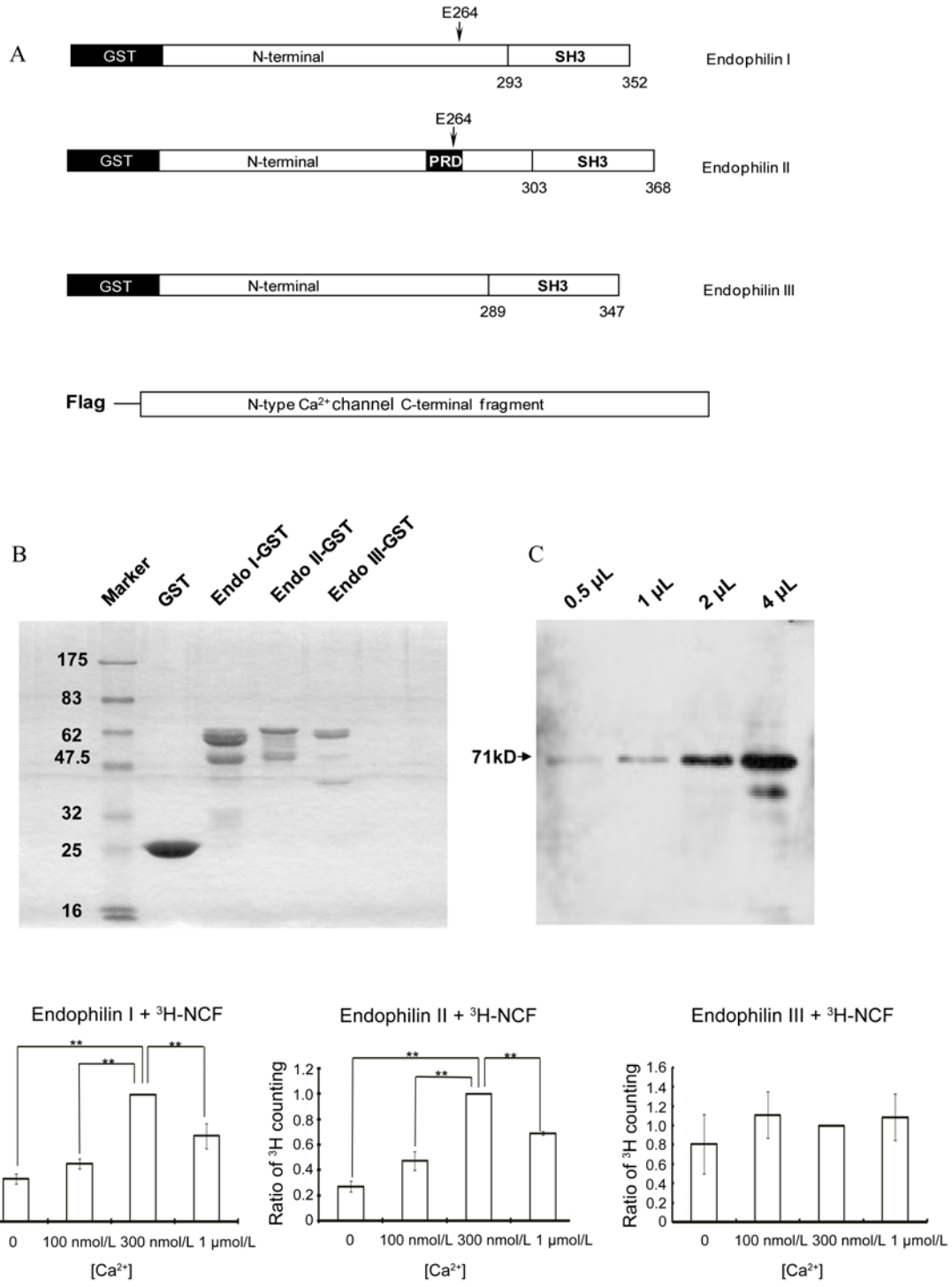

Fig. 1. Structures for endophilin and endophilin-GST pulldown assays. A: Schematic representations of GST-tagged endophilin I/II/III and pSP72-tagged N-type Ca^{2+} channel C-terminal fragment (NCF). Domain cartoons of the N-type Ca^{2+} channel C-terminal, endophilin PRD, E264 and SH3 domains are presented in proportion; numbers refer to the amino acids. B: Coomassie brilliant blue G-250-stained result of purified GST and GST-fused proteins of endophilin I/II/III. C: ^{3}H-leucine-labeled NCF detected by autoradiography. D: Pulldown assays of GST fusion proteins of endophilins and ^{3}H-labeled NCF were carried out at the indicated Ca^{2+} concentrations ($[Ca^{2+}]$). $n = 4$, $^{**}P < 0.01$, analyzed by one-way ANOVA followed by Bonferroni *post hoc* test.

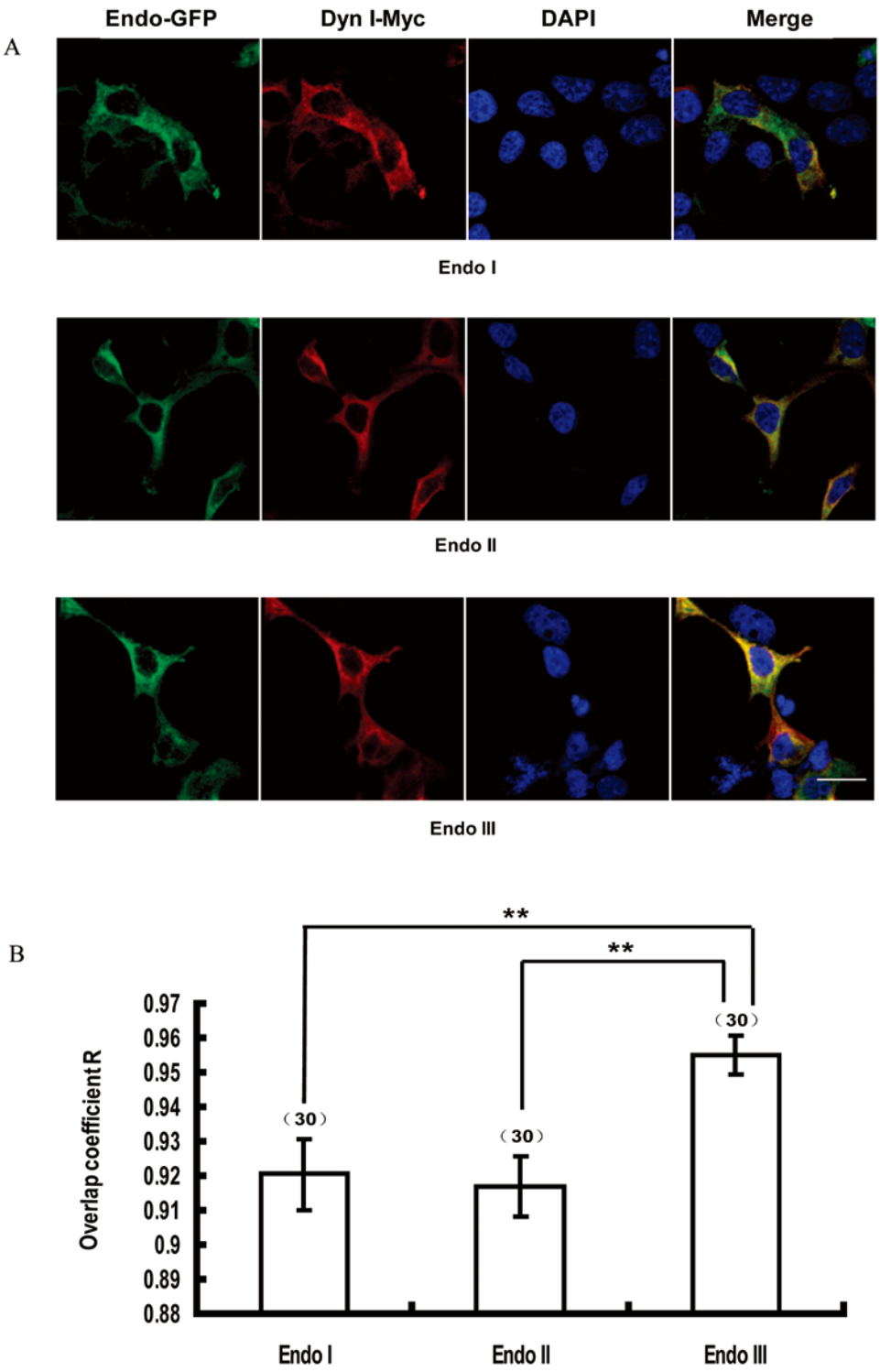

Fig. 2. Immunostaining of endophilin (Endo) isoforms and dynamin I (Dyn I) in 293T cells. A: Example images showing the colocalization of dynamin I (red) and endophilin I/II/III (green) in 293T cells. Scale bar, 20 μm. B: Summary data of the overlap coefficients of endophilin with dynamin I (n = 30). **P <0.01, analyzed by one-way ANOVA followed by Bonferroni *post hoc* test.

than that of endophilin III/GAPDH (I, 0.71 ± 0.03; II, 0.72 ± 0.08 *versus* III, 1.16 ± 0.07, P <0.01, n = 3, Fig. 3C). To avoid transfection efficiency affecting the results of protein expression, we used flow cytometry to investigate the co-localization of fixed 293T cells after double-staining. The data showed that colocalization of endophilin III with dynamin I was higher than endophilin I or endophilin II (Fig. 4A). Compared to endophilin II, the rate of colocalization increased from 55.23 ± 7.69% to 67.68 ± 1.01% (P <0.05, n = 3) in endophilin III (Fig. 4B). These results indicate that endophilin III had an enhanced interaction with dynamin I.

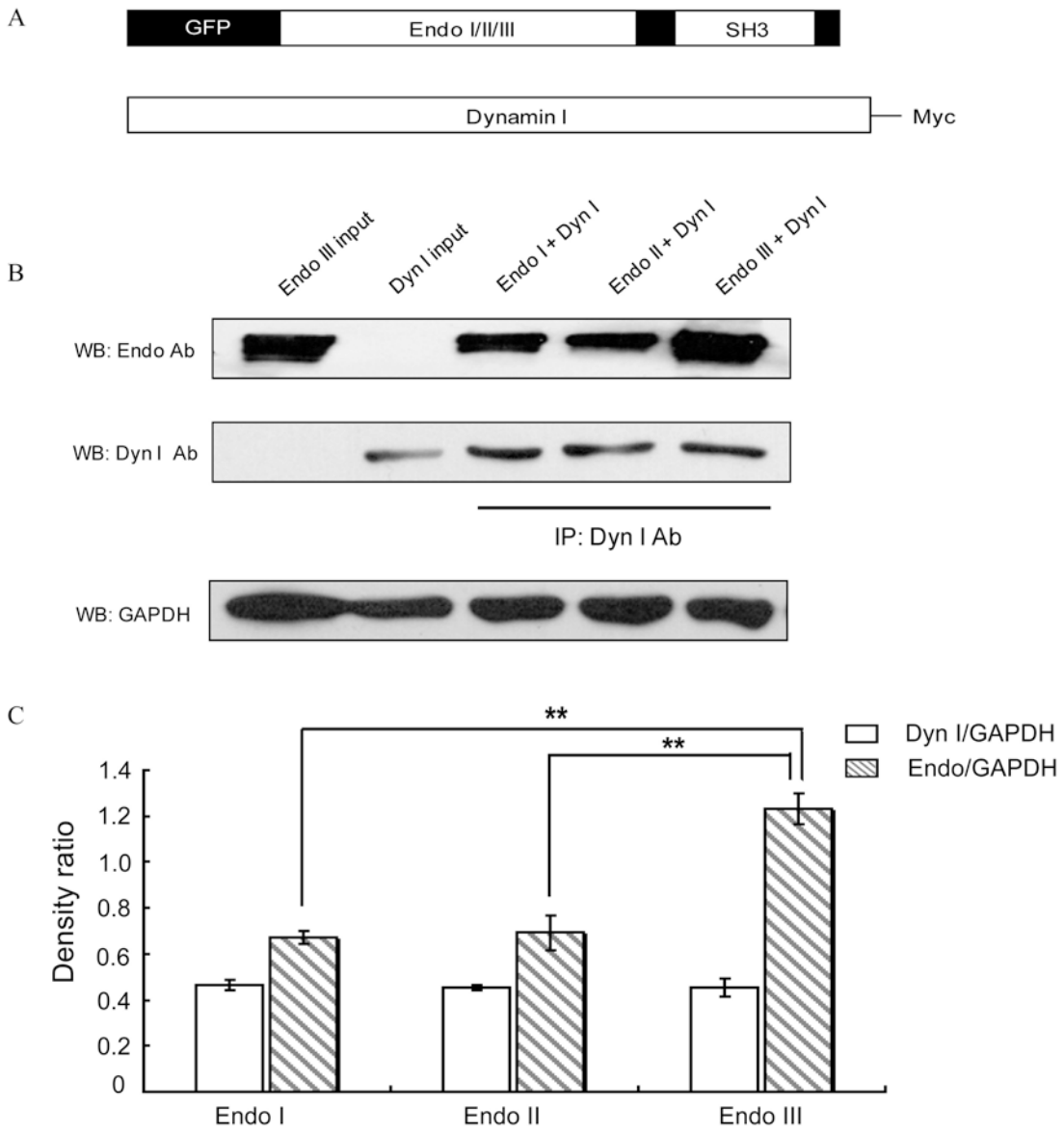

Fig. 3. Co-immunoprecipitation assays. A: Structural representations of GFP-tagged endophilin (Endo) I/II/III and Myc-tagged dynamin I. B: Forty-eight hours after transfection, 293T cell lysates were immunoprecipitated with dynamin antibody (Dyn Ab) and analyzed by immunoblotting. The blots were divided into three parts and each was probed with anti-dynamin, anti-endophilin or anti-GAPDH antibody. The first two lanes show endo philin/dynamin input. C: Density ratio of dynamin I or endophilin to GAPDH. Bars and error bars represent mean ± SE. All experiments were repeated at least three times (n = 3). **P <0.01, analyzed by one-way ANOVA followed by Tamhane *post hoc* test.

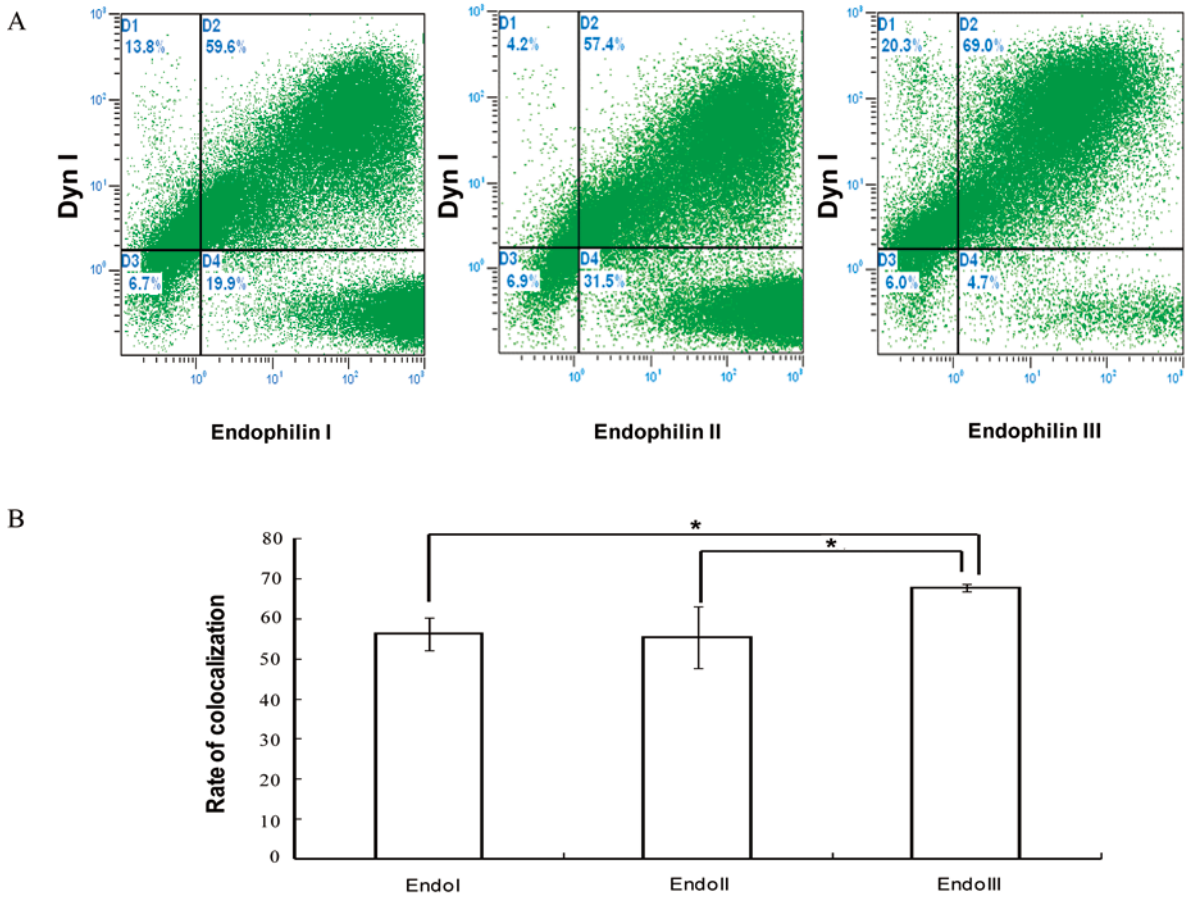

Fig. 4. Flow cytometric analysis of colocalization of endophilin I/II/III and dynamin I. Thirty-six hours after transfection, cells were stained with anti-PE antibody to evaluate the localization by flow cytometry. A: Different EGFP-endophilin isoforms interact with PE-dynamin (Dyn I). D1–D4 represent different groups of stained cells. Each number represents the binding percentage of endophilin with dynamin I (mean ± SE). B: One-way ANOVA test was used for statistical comparisons. The experiments were repeated three times (n = 3). *P <0.05, analyzed by one-way ANOVA followed by Tamhane *post hoc* test. Endo, endophilin.

4 Discussion

Our previous studies have shown that the formation of the endophilin II-channel complex is Ca^{2+}-dependent. The optimal [Ca^{2+}] for the binding of endophilin II to the Ca^{2+} channel is 100–300 nmol/L. When the concentration exceeds 1 μmol/L, the complex dissociates[23]. In this study, the binding of endophilin to NCF increased from 29.00 ± 4.25% to 100% as the [Ca^{2+}] was raised from 0 to 300 nmol/L, and decreased to 69.2 ± 1.55% when the [Ca^{2+}] was >1 μmol/L. These data are consistent with our previous study. The mechanism of Ca^{2+} regulation of endophilin II-NCF complex formation is based on the alternation of two endophilin II modes[23]. When [Ca^{2+}] is low (100–300 nmol/L), the endophilin II is in open mode and the SH3 domain can interact with dynamin and other proteins containing a PRD. As the [Ca^{2+}] increases, endophilin II switches to closed mode and blocks access to dynamin I or Ca^{2+} channels. It is reported that the resting [Ca^{2+}] in 293T cells is 50–100 nmol/L[30]. The co-IP results in 293T cells showed that endophilin II interacted with dynamin I and the colocalization ratio revealed by flow cytometric analysis was 55.23 ± 7.69%. In this situation, endophilin II is in open mode and can bind to dynamin I *via* its SH3 domain. It is unclear that whether Ca^{2+} regulates the interaction between

endophilin II and dynamin I. Our results indicate that Ca^{2+} might affect the binding of these two proteins by altering the endophilin II mode.

A similar phenomenon was found in the interaction of endophilin I with NCF. The Ca^{2+}-dependence of endophilin I-Ca^{2+} channel complex formation indicated that Ca^{2+}-binding sites exist within endophilin I. Glutamate 264 is one of the critical Ca^{2+} binding sites in endophilin II. Sequence analysis showed that glutamate 264 is conserved in endophilin I (P****E in endophilin I *versus* P**P*E in endophilin II). We suggest that this E264 might mediate the Ca^{2+}-dependent formation of the endophilin I-Ca^{2+} channel complex. The immunostaining and co-IP assays showed that endophilin I also interacted with dynamin, similar to endophilin II, in living cells. The flow cytometric analysis showed that the colocalization of endophilin I and dynamin was 56.15 ± 4.14%, close to that of endophilin II. As there is no PRD in endophilin I, the E264 might not be the only Ca^{2+}-binding site within endophilin I. There may be other Ca^{2+}-binding sites that are not involved in the PRD. Our data imply that the mechanisms of Ca^{2+} regulation of the formation of the endophilin-NCF complex differ between endophilin I and endophilin II.

Endophilin III interacted with NCF, but independently of Ca^{2+}. Its colocalization with dynamin I was stronger than endophilin I/II as revealed by immunostaining and overlay coefficient assays; both co-IP and flow cytometry showed that endophilin III had a greater ability to interact with dynamin I, the interaction ratio in living cells reaching 67.68 ± 1.01%. Due to the absence of the corresponding 260–272aa sites compared to endophilin I/II, endophilin III has neither a PRD nor an E264 Ca^{2+}-binding site. According to previous studies, the binding of Ca^{2+} to endophilin II E264 increases the affinity of the atypical PRD for the SH3 domain in endophilin II. The lack of PRD and E264 in endophilin III allows its SH3 domain to completely bind to dynamin. Besides, endophilin I/II are found as dimers through a coiled-coil domain in their conserved N-BAR moiety[30]. Not as much is known about the dimers of endophilin III. The structural information indicates that endophilin III might have more conformational space to bind to other proteins such as dynamin[4-7].

Formation of the endophilin II-channel complex is critical for clathrin-medicated synaptic vesicle endocytosis in neurons. Endophilin I had similar characteristics in interacting with the N-type Ca^{2+} channel and dynamin I. Compared with endophilin I/II, endophilin III had no Ca^{2+}-dependence in binding to NCF and demonstrated a greater ability to bind with dynamin I. Endophilins I and II are mostly concentrated at presynaptic terminals. Chowdhury *et al.* reported that endophilin III is concentrated equally at presynaptic terminals and postsynaptic spines, and endophilin III and dynamin interact with Arc/Arg3.1 to regulate AMPA receptor trafficking[32]. Accordingly, we suggest that endophilin III plays more important roles in the postsynaptic membrane than in presynaptic terminals. Taken together, the present study indicates that the three endophilin isoforms have different characteristics of interacting with associated proteins, indicating their distinct roles in clathrin-mediated endocytosis.

Acknowledgements: This work was supported by grants from the National Natural Science Foundation of China (30870785) and the Natural Science Foundation of Guangdong Province, China (9351008901000003).

References:

[1] Giachino C, Lantelme E, Lanzetti L, Saccone S, Bella Valle G, Migone N. A novel SH3-containing human gene family preferentially expressed in the central nervous system. Genomics 1997, 41: 427–434.

[2] Ringstad N, Nemoto Y, De Camilli P. The SH3p4/Sh3p8/SH3p13 protein family: binding partners for synaptojanin and dynamin via a Grb2-like Src homology 3 domain. Proc Natl Acad Sci U S A 1997, 94: 8569–8574.

[3] Reutens AT, Begley CG. Endophilin-1: a multifunctional protein. Int J Biochem Cell Biol 2002, 34: 1173–1177.

[4] Gortat A, Jouve San-Roman M, Vannier C, Schmidt AA. Single point mutation in the bin/amphiphysin/RVS (BAR) sequence of endophilin impairs dimerization, membrane shaping, and SRC homology 3 domain-mediated partnership. J Biol Chem 2012, 287(6): 4232–4247.

[5] Pawson T. Protein modules and signalling networks. Nature 1995, 373: 573–580.

[6] Ringstad N, Nemoto Y, De Camilli P. Differential expression of endophilin 1 and 2 dimers at central nervous system synapses. J Biol Chem 2001, 276: 40424–40430.

[7] Ross JA, Chen Y, Muller J, Barylko B, Wang L, Banks HB, *et al.* Dimeric endophilin A2 stimulates assembly and GTPase activity of dynamin 2. Biophys J 2011, 100: 729–737.

[8] Simpson F, Hussain NK, Qualmann B, Kelly RB, Kay BK, McPherson PS, *et al.* SH3-domain-containing proteins function at distinct steps in clathrin-coated vesicle formation. Nat Cell Biol 1999, 1: 119–124.

[9] Rikhy R, Kumar V, Mittal R, Krishnan KS. Endophilin is critically required for synapse formation and function in *Drosophila melanogaster*. J Neurosci 2002, 22: 7478–7484.

[10] Schuske KR, Richmond JE, Matthies DS, Davis WS, Runz S, Rube DA, *et al.* Endophilin is required for synaptic vesicle endocytosis by localizing synaptojanin. Neuron 2003, 40: 749–762.

[11] Hughes AC, Errington R, Fricker-Gates R, Jones L. Endophilin A3 forms filamentous structures that colocalise with microtubules but not with actin filaments. Brain Res Mol Brain Res 2004, 128: 182–192.

[12] Ringstad N, Gad H, Low P, Di Paolo G, Brodin L, Shupliakov O, *et al.* Endophilin/SH3p4 is required for the transition from early to late stages in clathrin-mediated synaptic vesicle endocytosis. Neuron 1999, 24: 143–154.

[13] Guichet A, Wucherpfennig T, Dudu V, Etter S, Wilsch-Brauniger M, Hellwig A, *et al.* Essential role of endophilin A in synaptic vesicle budding at the *Drosophila* neuromuscular junction. EMBO J 2002, 21: 1661–1672.

[14] Mizuno N, Jao CC, Langen R, Steven AC. Multiple modes of endophilin-mediated conversion of lipid vesicles into coated tubes: implications for synaptic endocytosis. J Biol Chem 2010, 285: 23351–23358.

[15] Gad H, Ringstad N, Low P, Kjaerulff O, Gustafsson J, Wenk M, *et al.* Fission and uncoating of synaptic clathrin-coated vesicles are perturbed by disruption of interactions with the SH3 domain of endophilin. Neuron 2000, 27: 301–312.

[16] Verstreken P, Kjaerulff O, Lloyd TE, Atkinson R, Zhou Y, Meinertzhagen IA, *et al.* Endophilin mutations block clathrin-mediated endocytosis but not neurotransmitter release. Cell 2002, 109: 101–112.

[17] Micheva KD, Kay BK, McPherson PS. Synaptojanin forms two separate complexes in the nerve terminal. Interactions with endophilin and amphiphysin. J Biol Chem 1997, 272: 27239–27245.

[18] Anggono V, Robinson PJ. Syndapin I and endophilin I bind overlapping proline-rich regions of dynamin I: role in synaptic vesicle endocytosis. J Neurochem 2007, 102: 931–943.

[19] Verstreken P, Koh TW, Schulze KL, Zhai RG, Hiesinger PR, Zhou Y, *et al.* Synaptojanin is recruited by endophilin to promote synaptic vesicle uncoating. Neuron 2003, 40: 733–748.

[20] Sundborger A, Soderblom C, Vorontsova O, Evergren E, Hinshaw JE, Shupliakov O. An endophilin-dynamin complex promotes budding of clathrin-coated vesicles during synaptic vesicle recycling. J Cell Sci 2011, 124: 133–143.

[21] Lee SY, Wenk MR, Kim Y, Nairn AC, De Camilli P. Regulation of synaptojanin 1 by cyclin-dependent kinase 5 at synapses. Proc Natl Acad Sci U S A 2004, 101: 546–551.

[22] McPherson PS, Garcia EP, Slepnev VI, David C, Zhang X, Grabs D, *et al.* A presynaptic inositol-5-phosphatase. Nature 1996, 379: 353–357.

[23] Chen Y, Deng L, Maeno-Hikichi Y, Lai M, Chang S, Chen G, *et al.* Formation of an endophilin-Ca^{2+} channel complex is critical for clathrin-mediated synaptic vesicle endocytosis. Cell 2003, 115: 37–48.

[24] Adler J, Parmryd I. Quantifying colocalization by correlation: the Pearson correlation coefficient is superior to the Mander's overlap coefficient. Cytometry A 2010, 77: 733–742.

[25] Zinchuk V, Wu Y, Grossenbacher-Zinchuk O, Stefani E. Quantifying spatial correlations of fluorescent markers using enhanced background reduction with protein proximity index and correlation coefficient estimations. Nat Protoc 2011, 6: 1554–1567.

[26] Chen-Hwang MC, Chen HR, Elzinga M, Hwang YW. Dynamin is a minibrain kinase/dual specificity Yak1-related kinase 1A substrate. J Biol Chem 2002, 277: 17597–17604.

[27] Yoshida Y, Kinuta M, Abe T, Liang S, Araki K, Cremona O, *et al.* The stimulatory action of amphiphysin on dynamin function is dependent on lipid bilayer curvature. EMBO J 2004, 23: 3483–3491.

[28] Hill E, van Der Kaay J, Downes CP, Smythe E. The role of dynamin and its binding partners in coated pit invagination and scission. J Cell Biol 2001, 152: 309–323.

[29] Szaszak M, Gaborik Z, Turu G, McPherson PS, Clark AJ, Catt KJ, *et al.* Role of the proline-rich domain of dynamin-2 and its interactions with Src homology 3 domains during endocytosis of the AT1 angiotensin receptor. J Biol Chem 2002, 277: 21650–21656.

[30] Aulestia FJ, Redondo PC, Rodriguez-Garcia A. Two distinct calcium pools in the endoplasmic reticulum of HEK-293T cells. Biochem J 2011, 435: 227–235.

[31] Weissenhorn W. Crystal structure of the endophilin-A1 BAR domain. J Mol Biol 2005, 351: 653–661.

[32] Chowdhury S. Arc/Arg3.1 interacts with the endocytic machinery to regulate AMPA receptor trafficking. Neuron 2006, 52: 445–459.